Unclassified

SECURITY CLASSIFICATION OF THIS PAGE *(When Data Entered)*

REPORT DOCUMENTATION PAGE		READ INSTRUCTIONS BEFORE COMPLETING FORM
1. REPORT NUMBER 1-83	2. GOVT ACCESSION NO.	3. RECIPIENT'S CATALOG NUMBER
4. TITLE *(and Subtitle)* Optical Sound Generation and Amplification		5. TYPE OF REPORT & PERIOD COVERED Annual Summary 6. PERFORMING ORG. REPORT NUMBER
7. AUTHOR*(s)* Henry Bass, Lawrence Crum, and F. Douglas Shields		8. CONTRACT OR GRANT NUMBER*(s)* N00014-81-K-0691
9. PERFORMING ORGANIZATION NAME AND ADDRESS Physical Acoustics Research Laboratory Department of Physics The University of Mississippi, University, MS 38677		10. PROGRAM ELEMENT, PROJECT, TASK AREA & WORK UNIT NUMBERS NR 384-836
11. CONTROLLING OFFICE NAME AND ADDRESS Office of Naval Research, Physics Division Code 412, Artlington, VA 22217		12. REPORT DATE 1-15-83 13. NUMBER OF PAGES
14. MONITORING AGENCY NAME & ADDRESS*(if different from Controlling Office)*		15. SECURITY CLASS. *(of this report)* Unclassified 15a. DECLASSIFICATION/DOWNGRADING SCHEDULE

16. DISTRIBUTION STATEMENT *(of this Report)*

Approved for public release; distribution unlimited.

17. DISTRIBUTION STATEMENT *(of the abstract entered in Block 20, if different from Report)*

18. SUPPLEMENTARY NOTES

19. KEY WORDS *(Continue on reverse side if necessary and identify by block number)*

Acommodation coefficients
Acoustic cavitation
Optoacoustic effect

20. ABSTRACT *(Continue on reverse side if necessary and identify by block number)*

This report is an annual summary report on various tasks associated with a general study of optical sound generation and amplification in fluids.

DD FORM 1 JAN 73 1473 EDITION OF 1 NOV 65 IS OBSOLETE

S/N 0102-LF-014-6601

Unclassified

SECURITY CLASSIFICATION OF THIS PAGE *(When Data Entered)*

[redacted]

THE UNIVERSITY OF MISSISSIPPI
PHYSICAL ACOUSTICS RESEARCH GROUP
DEPARTMENT OF PHYSICS AND ASTRONOMY

Annual Summary Report

for

Office of Naval Research

Contract N00014-81-K-0691

Optical Sound Generation and Amplification

1-83

by

Henry Bass, Lawrence Crum and F. Douglas Shields
Physical Acoustics Research Laboratory
Department of Physics and Astronomy
The University of Mississippi
University, Mississippi 39677

January 15, 1983

Task I

Modulation of Light for Optical Generation of Sound

by

Henry E. Bass

This task is devoted to optical generation of sound at audible frequencies. The optical source of energy must be modulated to produce a time dependent heating and this time dependent heating is then converted to a pressure variation. We have been considering conversion from light to sound in a gas (classical spectrophone) and at a surface (as observed by Alexander G. Bell). Our efforts during the past year have been devoted to:

1. Developing the theory of sound conversion at a surface, preparing surfaces, and preliminary measurements to compare with theory. Our results to date are summarized in Appendix A which follows.

2. Developing a theory which describes transfer of energy to a pressure pulse in a gas (similar to the liquid problem) and comparison of predictions to experiment. The theory is described in Appendix B; experimental results have not been completely analyzed.

3. Continuing study of sound amplification in a reacting gas.

We have also made progress in the study of pulse density modulation as a means of converting a string of rapid pulses to an acoustic signal (see Appendix C attached).

APPENDIX I-A

Generation of Sound at a Surface Subjected to Modulated Light

Introduction

Generation of acoustic waves by absorption of electromagnetic radiation indicent on a surface was first reported by Bell.[1] More recently, this technique has been adapted to studies of surface absorption coefficients.[2] The possibility of exploiting this phenomena as a means of generating ultrasound for communications purposes was raised by Westervelt and Larson.[3] They treated the case where thermal conduction can be ignored which is true at very high frequencies in water. Their result yields small conversion efficiencies except at very high frequencies. Temkin[4] treats the case of a flat surface with its temperature moldulated and concludes that the efficiency for conversion of evergy into sound is proportional to $\omega^{\frac{1}{2}}$ with a value near 10^{-5} at 10Hz. This would imply that a 100 watt light bulb turned on and off at 10 Hz would provide a sound pressure level of 125 dB in air. This is not the case. The reason for the descrepancy lies in the neglect of the energy required to maintain an average energy flow away from the surface.

In the following, we will treat sound generation at the surface of a plate coated with a very thin layer of optically absorbing material (lamp black or AlO_2). We will be interested in the audible frequency range particularly the low end of this range ($\sim$10 Hz).

Theory

From Reference 4, writing the temperature of the abosrbing surface as

$$T_w = T_o + \varepsilon \cos \omega t \tag{1}$$

and assuming that there is no heat flow out of the rear plate, the acoustic intensity becomes

$$I = \tfrac{1}{2} \rho_o \omega \kappa_o c_o \beta_o^2 \varepsilon^2 \tag{2}$$

where κ_o is the thermal diffusivity, c_o is the speed of sound, and β_o is the coefficient of thermal expansion which takes on the value $1/T_o$ for an ideal gas.

Burdick and Arnold[5] have solved for the temperature fluctuations in a thin film absorbing modulated radiation of the form

$$I_\ell(t) = I_o/2(1-e^{j\omega t}). \tag{3}$$

They write the energy balance equation in the form

$$\alpha I = C_p \rho \ell (dT^*/dt) + BT^* \tag{4}$$

where α is the fraction of the radiation sbsorbed, $(C_p \rho \ell)$ is the specific heat of the absorbing surface, T* is the difference between the surface temperature and the temperature of the surroundings and B is the effective thermal conductance. The effective thermal conductance is the power transported from the surface (unit area $-°K)^{-1}$. This can be related to the thermal conductivity of the gas, by

$$B = k_o/\delta_o \tag{5}$$

where δ_o is the distance in the gas necessary to establish the temperature difference T*, and k_o is the thermal conductivity of the gas.

Eq. (4) has a solution

$$T^*(t) = \frac{\alpha I_o}{2B} - \frac{\alpha I_o \exp(j\omega t)}{2(B+j\omega C_p \rho \ell)} . \tag{6}$$

For the purposes of Eq. (2), we are interested only in the real part of the oscillating term in Eq. (6), $T^*_{a.c.}(t)$, so

$$T^*_{a.c.}(t) = \frac{-\alpha I_o}{2} - \frac{(B \cos \omega t + \omega C_p \rho \ell \sin \omega t)}{[B^2 - \omega^2 (C_p \rho \ell)^2]} . \tag{7}$$

We see that in Eq. (7), there are two oscillating terms, each will be dominant

for different ranges of frequencies. Prior to examining the intensity, we will establish the limiting conditions on Eq. (7).

We will assume δ_o is the thickness of the thermal layer near the surface which is given by $2\pi(2\kappa_o/\omega)^{\frac{1}{2}}$ so

$$B = \frac{k_o}{2\pi}\left(\frac{\omega}{2\kappa_o}\right)^{\frac{1}{2}} = \frac{1}{2\pi}\left(\frac{\omega}{2}\rho_o C_{po} k_o\right)^{\frac{1}{2}}. \tag{8}$$

If we let $\rho_o C_{po} = 2.83 \times 10^{-4}$ cal $(cm^3K)^{-1}$, and $k_o = 6.22 \times 10^{-5}$ cal $(cm^3 sec\ K)^{-1}$ which are values for N_2 at 300K,

$$B \simeq 1.5 \times 10^{-5} \text{ cal } (cm^3K)^{-1}(\omega/sec)^{\frac{1}{2}}. \tag{9}$$

The quality $(C_p\rho\ell)$ is more difficult to estimate since our surface is less well understood. We will adopt C_p for gold from our experiment (see next section) which gives $C_p\,\rho\ell \simeq 3.6 \times 10^{-3}$ cal $(cm^2K)^{-1}$. Eq. (7) becomes

$$T^*_{a.c.}(t) = \frac{-\alpha I_o}{2\omega}\left[\frac{1.5 \times 10^{-5}(\omega/sec)^{\frac{1}{2}}\cos\omega t + 3.6 \times 10^{-3}\sin\omega t}{2.25 \times 10^{-10}/sec - \omega \cdot 2.3 \times 10^{-5}}\right] cal^{-1}(cm^2K) \tag{10}$$

We see that except near $\omega = 0$,

$$T^*_{a.c.}(t) \simeq + \frac{\alpha I_o \sin\omega t}{2\omega\, C_p\rho\ell}\ . \tag{11}$$

The sin ωt term indicates that the variation in gas temperature is 90° out of phase with the light source.

We can now rewrite Eq. (2) as

$$I = \frac{1}{8}\alpha^2 I_o{}^2 \frac{\rho_o \kappa_o c_o}{T_o^2 (C_p\rho\ell)^2}\frac{1}{\omega} \tag{12}$$

recognizing that when $\omega \to 0$, Eq. (11) is no longer valid. Writing $\kappa_o = k_o/\rho_o C_{po}$,

$$I = \frac{1}{8}\ \alpha^2 I_o{}^2 \frac{k_o c_o}{C_{po} T_o{}^2}\ \ \frac{1}{(C_p\rho\ell)^2}\ \frac{1}{\omega} \tag{13}$$

or, assuming plane waves,

$$p = \tfrac{1}{2}\,\alpha I_o c_o / T_o (C_p \rho \ell) \cdot (k_o \rho_o / 2C_{po}\omega)^{\frac{1}{2}}. \tag{14}$$

It is interesting to note that the acoustic intensity goes as the square of the optical intensity. Since we have assumed plane waves, this means that the acoustic pressure is proportional to I_o and inversely proportional to $\omega^{\frac{1}{2}}$.

This result can now be compared to the results of Roscenwaig and Gersho[2] and Parker.[6] Roscenwaig and Gersho treated the more complete problem of a finite backing plate and an absorbing surface of finite thickness. If we let the surface thickness approach zero, assume all the energy is absorbed, and the plate has a small thermal conductivity, their result can be written as

$$\delta p(t) = Q e^{j(\omega t - \pi/4)} \tag{15}$$

where

$$Q = \frac{\gamma P_o}{2^{1/2} \ell_g a_g T_o} \; \frac{\beta I_o}{2k_s(\beta^2 - \sigma_s^2)} \left[\frac{(1-j)\beta k_s}{2k_g \alpha_b \alpha_s^2/\alpha_g}\right], \tag{16}$$

ℓ_g is the length of the test cell (they assume a finite length), β is the absorption coefficient which we assume to be large, k_s and k_g are the thermal conductivities of the surface and gas respectively, α_b, α_s and α_g are the thermal diffusivities of the backing plate, surface, and gas respectively, $a_g = (\omega/2\alpha_g)^{\frac{1}{2}}$, and $\sigma_s = (1+j)(\omega/2\alpha_s)^{\frac{1}{2}}$. Substituting and cancelling terms,

$$Q = \frac{\gamma P_o \beta^2 I_o}{4\ell_g T_o} \; \frac{(1-j)}{(\beta^2 + j\omega/\alpha_s)} \; \frac{1}{k_g \alpha_b \alpha_s^2/\alpha_g^{\frac{1}{2}}} \; \frac{1}{\omega^{\frac{1}{2}}} \quad . \tag{17}$$

Since we have assumed β^2 is large,

$$Q \simeq \frac{\gamma P_o I_o}{4\ell_g T_o} \; \frac{(1-j)}{k_g \alpha_b \alpha_s^2/\alpha_g^{\frac{1}{2}}} \; \frac{1}{\omega^{\frac{1}{2}}} \tag{18}$$

Although the expression is quite approximate due to the assumptions made, we note that $\delta P \propto \omega^{-\frac{1}{2}}$ which is consistent with the earlier finding that $I \propto \omega^{-1}$. Also, $\delta P \propto I_o/T_o$ consistent with our earlier result.

For a fixed length cell, Parker finds, for the pressure midway in the cell,

$$P\ (\ell/2) = -\left[\frac{\gamma-1}{2c_o \sin(k_o \ell/2)}\right]\left[j\left(\frac{C_{po} k_o}{\omega}\right)\right]^{\frac{1}{2}}\left(\frac{\alpha I_o}{c_{po}}\right) . \qquad (19)$$

Again, δ_p is proportional to $\omega^{-\frac{1}{2}}$ and I_o but there is a difference between Eq. (20) and Eq. (13) in the way that C_{po} enters. Parker finds that $\delta p \alpha C_{po}^{\frac{1}{2}}$; Eq. (13) gives $\delta p \alpha C_{po}^{-\frac{1}{2}}$. This descrepancy arises in the application of the boundary condition at x and ℓ.

For an absorbing liquid ignoring thermal conduction, Westervelt and Larson have shown that the total acoustic power generated is

$$W = \alpha\omega\beta^2 P_o^2/16\rho_o C_{po}^2$$

where β is the coefficient of thermal expansion and α is the attenuation coefficient for the light source. Note that in this case, W is proportional to ω.

Experimental

Referring to Eq. (13), if one wishes to generate sound in air (our initial goal), the parameters which can be controlled are α, the fraction of absorbed incident radiation, I_o, the incident intensity, $C_p\rho\ell$, the specific heat of the absorbing material, and ω, the frequency of modulation. Each of these parameters have been explored.

For experimental purposes, the surface which we can most readily control is AlO_x and AuO_x. Several surfaces were prepared with both Al and Au vacuum depostied on 4 x 4 x $\frac{1}{4}$ inch glass plates. The amount of metal was controlled by placing different amounts of metallic wire in the bell jar. By placing a shield around the melting wire, an estimate of the fraction of metal ending up on the plate was determined. In addition, the surface resistance was measured giving another indication of surface thickness. The amount of oxidation was controlled by varying the pressure in the bell jar when the metal was heated and the rate at which the metal melted. Our goal was to achieve maximum absorption at the surface (incident intensity/transmitted intensity) with minimum metal (thereby minimizing $C_p\rho\ell$).

The metal wire to be melted was attached to a tungsten filament. The tungsten filament was heated by controlling the current. Several problems were encountered which made the resultant coating only partially reproducible. First, if any metal remained on the filament from one attempt to the next, more metal was available for coating and the surface would sometimes be thicker. When the tungsten filament was heated, the pressure inside the bell jar proved very difficult to control thus giving non-repeatable levels of oxidation. Heating the tungsten filament in the presence of oxygen also caused the filament to oxidize leading to a very short lifetime. All these problems are associated with vacuum deposition in a reactive atmosphere.

A sufficiently large number of surfaces were prepared to give us a reasonable range of α and $(C_p \rho \ell)$. The conditions for the gold black furface are given in Table I. Each piece of gold wire has a specific heat of approximately 2.3 joule/°K. For an average filament to plate distance, 5/8 of the gold ended on the plate so the total specific heat of the gold deposited was about 1.5 Joule/°K. The plates have an area of $0.01 m^2$. However, if in the future we wish to optimize the surface, more work must be done in controlling the deposition process. The surfaces and deposition conditions are given in Table I.

The intensity of the incident radiation and frequency were varied in two ways. First, a Gen Rad 1531 AB Stroboscope was used as a light source. This source delivers a pulse; the duration and energy can be selected from three combinations: 0.8 μs, 6×10^5 candela; 1.2 μs, 3.5×10^6 candela; or 3.0 μs, 1.1×10^7 candela. The capacitors in the stroboscope emit a loud click when discharging so this unit was mounted in a box with a plexiglass window. The glass plate with the light absorbing surface was placed in a second box with another plexiglass window to let in light. A B&K ½" microphone was placed in the box with the abosrbing plate.

Typical waveforms for the measured acoustic signal are given as Figure 1.

It is now of interest to compare our experimental observations to predictions. First, referring to Figure 1, we note that the period of the wave is not very sensitive to the length of the incident light pulse. This resulting pulse scales in pressure approximately linearly with the total power of the pulse, in accordance with Eq. (14). Substituting estimated values for the specific heat of the surface (used earlier as an example) and assuming a fundamental frequency of 5 kHz, gives $p \cong 1.0 \times 10^{-4}$ Pa. Our experimental result gives a value of $p \cong 1.0 \times 10^{-1}$ Pa. We are not now in a position to determine the origin of this order of magnitude discrepancy. Assuming the theory is cor-

rect, the most uncertain quantity in Eq. (14) is $(C_p \rho \ell)$. We have used the value for gold which is quite likely much different than gold oxide. Further, we assumed that 5/8 of the gold wire found the plate. This fraction could be as low as 1/8. Future experiments to narrow this descrepancy will require a more careful characterization of the surface.

Conclusions

At this time, we are not yet in a position to determine how accurately Eq. (14) describes the sound generation process. This relation will allow us to reach tentative conclusions concerning the viability of this process for generating acoustic energy. Referring to Eq. (14), we have no control of T_o, k_o, ρ_o, or C_{po}. This leaves I_o, the incident power, $(C_p \rho \ell)$ the specific heat of the surface, and ω, the frequency.

In order to reconcile experiment and theory, we have to assume that $C_p \rho \ell \simeq 1.1 \times 10^{-4}$ cal $(\text{cm K})^{-1}$ which would imply a film thickness $\sim 2\mu$. Our experience suggests that films of gold black less than $\sim 0.5\mu$ will become transparent. This means that $C_p \rho \ell$ can be reduced at most by a fraction of 4 using gold black. Such a reduction would give an acoustic pressure of ~ 1.6 Pa (98 dB) at 5 kHz.

The frequency dependence in Eq. (1) suggests that this method of generating sound is most useful at low frequencies. By decreasing the frequency to 50 Hz, the SPL will increase by 20 dB. This result is quite interesting since conventional sound sources tend to be least effective at low frequencies.

The input power dictates the resultant SPL as one would expect. In order to generate 80 dB, 2.8×10^3 watts/m^2 is required. To generate sound over an area of 0.1 m^2 280 watts of optical energy would be required. This is an order of magnitude higher than convential sound sources. Assuming we can generate an absorbing layer of gold black 0.5μ thick, at 50 Hz, then 280 watts will produce a SPL of 118 dB which is comparable to convential sources. At lower frequencies, opto-acoustic conversion should be more efficient than convential mechanical speakers.

The above suggests that with our present surfaces opto-acoustic generation of sound in air will be useful only when

a. sound needs to be introduced into a region where it is not feasible to place mechanical drivers or run power cords (vacuum systems, low EMI test regions, fiber optic communication links, etc.);

b. a low frequency ($\sim$50 Hz) sound source is required but tuned air horns are not feasible.

Our major effort, then, must be to reduce the specific heat of our light absorbing surface. Before doing so, we plan to explore Eq. (14) more thoroughly to determine the range of validity.

Table I

Characteristics of Light Absorbing Plates

(Gold Black)

Plate #	Starting Pressure	Amount of Wire	Transmission of Surface	Appearance of Surface	Comments
#1	50μ	1 piece 1 cm 0.039g	Very transparent coat About 1/2 transmission	Gold-black edges with darker spot in middle	The time needed to vaporize varies.
#2	70-80μ	2 pieces 1 cm each 0.078g	Very little transmission No reflection	Golden brown spot in middle, darker black edges	
#3	80μ	3 pieces 2/3 cm each 0.078g	Glass almost as it was before coating	Very little coating	Filament is 2 1/2" higher from plate than normal.
#4	80μ	3 pieces 2/3 cm each 0.078g	Center is clearer than edges; edges high transmission	Edges are blue-black No reflection	Filament is 1" - 1 1/2 " higher from plate than normal
New filament 1/2 as long as filament #1					
#5	70-80μ	2 pieces 1 cm each 0.078g	Low transmission	Golden black center with streaks; very reflective except streaks	Filament 1 1/2" off plate
#6	70-80μ	3 pieces 1 cm each 0.078g	Transmission is low where coat is thick; not as reflective as #5	Black streaks with surface colors varying from gold to brown to blue to black	Filament was 2 1/2" off plate
#7	80μ	2 pieces 1 cm each 0.078g	No transmission, especially at center	1st coat was shiny (reflective) surface; 2nd coat thicker nonreflective coat very black center; small gold streaks are reflective	Filament 2 1/2" off plate At 15V for 3 min. 1 piece melted; at 30-40V for 1 min other piece melted.

Diameter of wire - 0.0508 cm

#2, #7 are the "loudest" plates

Table II

Characteristics of Stroboscope

Strobe Speed Setting	High	Medium	Low
Pulse Length (μsec)	0.8	1.2	3.0
Luminous Intensity (Cd)*	0.6×10^6	3.5×10^6	11×10^6
Power of Pulse (total, watts/m^2)	1.5×10^2	8.8×10^2	2.8×10^3
Energy/pulse (J/m^2)	1.2×10^{-4}	1.0×10^{-3}	8.4×10^{-3}
Acoustic pressure (Pa)	--	$22/-15 \times 10^{-3}$	$150/-110 \times 10^{-3}$

*Beam Width - 10° = 0.17 Steradians

Figure 1

Typical Waveforms

18 Nov 82
Stroboscope: 690 RPM
Rockland Filter:
Low pass 80KHz
High pass 300 Hz
Gain 20 dB

Oscilloscope:
Vertical 0.1 v/div
Horizontal 0.2 msec/div

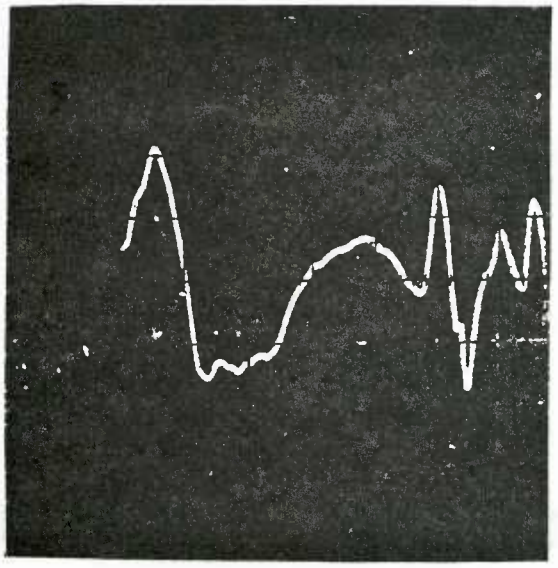

10 Nov 82
Stroboscope: 4170 RPM
Rockland Filter:
Low pass 80KHz
High pass 300 Hz
Gain 20 dB

Oscilloscope:
Vertical 50 mv/div
Horizontal 0.2 msec/div

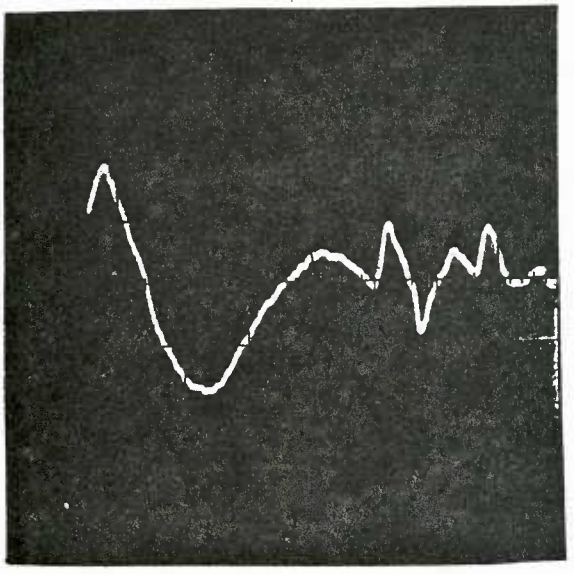

References

1. Alexander Graham Bell, Philosophical Magazine 11, 510 (1881).

2. Allan Rosencwaig and Allen Gersho, Science 190, 556-557 (1975).

3. Peter J. Westervelt and Richard S. Larson, J. Acoust, Soc. Am. 54, 121-122 (1973).

4. Samuel Temkin, "Elements of Acoustics", p. 472. (John Wiley & Sons, New York, 1981).

5. Glenn A. Burdick and Roy T. Arnold, J. Applied Physics 37, 3223-3226 (1966).

6. J.G. Parker, Applied Optics 12, 2974-2977 (1973).

APPENDIX I-B

The following pages represent appendices (draft form) to a paper being prepared on spectrophone measurements of vibrational energy transfer. Please note that the equation symbols and appendix letters correspond to the planned publication independent of this report.

Appendix A

Solution of Heat Flow Equations

The kinetic equations for the spectrophone response as a function of time have been solved by Bauer.[1] He assumed, however, that thermal conduction to the cell walls is very slow compared to the rate of collisional deactivation. In this case,

$$P(t) - P(o) = (P/nTC_v^{\infty}) \Sigma(\underset{\sim}{r}_i \underset{\sim}{u} \underset{\sim}{r}_i \underset{\approx}{x}^{-1} \underset{\sim}{n}_{ex})(1 - e^{-t/\tau^i_{vs}}) \qquad A1$$

where $\underset{\sim}{r}_i$ is the $i^{\underline{th}}$ right hand eigenvector of the matrix $[\underset{\sim}{\nu}\underset{\sim}{k}\underset{\sim}{\tilde{\nu}}(x^{-1} + \underset{\sim}{u}\underset{\sim}{\tilde{u}}/RC_v^{\infty}T^2)]$ as defined by Bauer, $\underset{\sim}{u}$ is a vector of energy states, $\underset{\sim}{\nu}$ is a matrix of stochiometric coefficients, $\underset{\approx}{x}^{-1}$ is a matrix with the inverse of the concentrations in the diagonal, C_v^{∞} is the non-relaxing specific heat, T is the temperature, $\underset{\sim}{n}_{ex}$ is a vector with the total excitation resulting from the input laser pulse for each energy state, t is time, and τ^i_{vs} is the relaxation time (eigenvalue) associated with the $i^{\underline{th}}$ eigenvector. This expression can be conveniently rewritten in the form

$$P(t) - P(o) = (P/nTC_v^{\infty})\Sigma\delta_i(1- e^{-t/\tau^i_{vs}}) \qquad A2$$

where δ_i is a relaxation strength.

For purposes of the experiment described here, thermal conductivity can not be ignored. The equation for heat flow in the cell can be written as[2]

$$\frac{\partial\theta}{\partial t} = \kappa\left(\frac{\partial^2\theta}{\partial r} + \frac{1}{r}\frac{\partial\theta}{\partial r}\right) + \Theta(r,t) \qquad A3$$

where θ is the difference between the gas and tube temperatures (the tube temperature is assumed to be constant). We will assume that the heat generation term $\theta(r,t)$ is a product of space dependent and time dependent parts,

$$\theta(r,t) = \frac{\kappa}{k} f(r)g(t)$$

where κ is the "thermal diffusivity" and k is the thermal conductivity ($k = \kappa C_v \rho$). The function g(t) is the heat generated by relaxation processes which, from A2 is

$$g(t) = \sum_i \delta_i (1 - e^{-t/\tau_{vs}^i}). \qquad \text{A5}$$

Actually Eq. A5 is more exact than A2 since the derivation leading to A2 assumes that the pressure change is transmitted to all parts of the cell instantaneously (acoustic transmit time is ignored).

Weulevesse and Genier[3] use the translational part of the thermal conductivities and heat capacities in Eq A3 then include diffusion of vibrational energy to the walls by adding another term. We will choose to consider diffusion of vibrational energy to the walls separately since, for our conditions, this effect is almost always negligible. Even though we consider diffusion of vibrational energy separately, we still use the equilibrium values of k and c_v even though these include vibrational contributions.

To a good approximation, $k = 5/3\ \eta\ (C_v/m)$ (Euken Approx.) which gives $\kappa = 5\eta/2m\rho$. This equation remains true without regard for the number of degrees of freedon (beyond translation) considered so the use of equilibrium values of κ and C_v will yield the same results in the important exponential term which follows as a more rigorous treatment based on k_{trans} and $C_{v,trans}$.

Prior to proceeding further with the solution of A3, a form for f(r) must be assumed. In the following, we will assume a uniform axial excitation (we have already assumed uniform excitation longitudinally) then we will assume

a Gaussian distribution across the cell radius.

Uniform Excitation

For uniform excitation, $f(r) = 1$ and

$$\theta(r,t) = \frac{2\kappa}{ka^2} \sum_n \frac{J_o(r\xi_n)}{[J_1(a\xi_n)]^2} \frac{a}{\xi_n} J_1(a\xi_n) \int_o^t g(t')e^{-\kappa\xi_n^2(t-t')}dt' \qquad A6$$

where ξ_n is a root of the equation $J_o(\xi_n a) = 0$ which arises from the condition that $\theta = 0$ when r equals the cell radius a and J_o, J_1 are Bessel's functions. Evaluating the integral over time gives

$$\theta(r,t) = \frac{2\kappa}{k} \sum_{n,i} \delta_i (\kappa\xi_n^2\tau_i - 1)^{-1}(e^{-t/\tau_i} - e^{-\kappa\xi_n^2 t}) \frac{J_o(r\xi_n)}{a\xi_n J_1(a\xi_n)} . \qquad A7$$

We now assume that the acoustic transit time is small compared to relaxation processes so the pressure observed is proportional to the average temperature rise across the cell radius where

$$\theta(t) = 2\pi \int_o^a \theta(r,t) r dr/\pi a^2. \qquad A8$$

Integrating gives

$$\theta(t) = \frac{4}{a^2} \frac{\kappa}{k} \sum_{n,i} \frac{\delta_i}{\xi_n^2} (\kappa\xi_n^2\tau_i - 1)^{-1} (e^{-t/\tau_i} - e^{-\kappa\xi_n^2 t}) \qquad A9$$

which is the desired result. Writing out the pressure dependent terms explicitly,

$$\theta(t) = \frac{4}{a^2} \frac{RT}{C_v p} \sum_{n,i} \frac{\delta i}{\xi_n^2} \left(\frac{RTk\xi_n^2\tau_i}{C_v p} - 1\right)^{-1} (e^{-t/\tau_i} - e^{-RTk\xi_n^2 t/C_v p}) \qquad A10$$

or

$$\theta(t) = \frac{4}{a^2} \sum_{n,i} \frac{\delta_i}{\xi_n^2} (k\xi_n^2\tau_i - \frac{C_v p}{RT})^{-1} e^{-RTk\xi_n^2 t/C_v p} \left(e^{-\left(\frac{1}{\tau_i} - RTk\xi_n^2/C_v p\right)t} - 1\right) \qquad A11$$

It can be seen from Eq. All that the effect of heat conduction is to make the effect deexcitation rate larger and pressure dependent and make the relaxation strength pressure and time dependent. We can see that even clearer if we write $RTk\xi_n^2/C_v p = 1/\tau_{tc}^n$ and $\frac{4}{a^2}\frac{\delta_i}{\xi_n^2}(k\xi_n^2\tau_i - \frac{C_v p}{RT})^{-1} = \Delta_{in}$ so Eq. All becomes

$$\theta(t) = \sum_{n,i}\Delta_{in}\, e^{-t/\tau_{tc}^n}(e^{-t(1/\tau_i - 1/\tau_{tc})} - 1). \qquad \text{A12}$$

In the proceeding, we have ignored energy transfer to the cell windows. Since that mechanism will always increase the energy loss, we would expect that τ_{tc}^n will be less than $(C_v p/RTk\xi_n^2)$. We have also ignored radiative transfer of energy to the cell walls. This will be considered next.

Ideally, heat transfer to the walls fo the tube would be included by introducing spontaneous emission into the relaxation equations. To do so introduces an inordinate degree of difficulty since the resultant matrices loose the symmetry which made an analytical solution possible. We choose to treat the effects of spontaneous emission less rigorously but in a manner which gives an analytical solution.

Spontaneous emission will have two experimentally observable effects. At high pressure, since the effects of thermal conduction decreases with increasing pressure, spontaneous emission is a mechanism for transferring the heat supplied to the gas by the laser to the cell walls. This effect will parallel thermal conduction and will be important for high gas pressures and long times. At low pressures, spontaneous emission will offer a parallel relaxation path to the slow collisional processes.

On a time scale much longer than required for collisional energy transfer, the vibrational modes are in equilibrium and can be described by a single temperature. In the absence of conduction or radiation losses, this temperature is given as

$$T_{gas} = T + (P/nTC_v^{\infty})\sum_i \tilde{r}_i \tilde{u}_{r_i} x^{-1} \tilde{n}_{ex} \qquad A13$$

where T is the temperature of the cell walls.

The rate of heat transfer per unit length to the walls of a cylinder of gas can be written approximately as[4]

$$Q = 4\pi\sigma\alpha_g T^3 \theta R \qquad A14$$

where σ is the Stefan-Boltzman constant, α_g is the absorption coefficient for the gas, θ is the difference between the gas and wall temperatures, and R is the cell radius. We have assumed that the absorption coefficient equals the emissivity and have ignored terms in θ^2 or greater.

The rate of change in temperature is given by

$$\dot{\theta} = \frac{-4\pi\sigma\alpha_g T^3 R \cdot \ell}{C_v^t}\theta \qquad A15$$

where ℓ is the cell length and C_v^t is the total heat capacity. In terms of the specific heat/unit volume,

$$\dot{\theta} = -\frac{\sigma\alpha_g T^3 \theta}{C_v R} \qquad A16$$

which has a solution

$$\theta = Ae^{-t/\tau_r} \qquad A17$$

where $\tau_r = C_v R/\sigma\alpha_g T^3$. Note that τ_r is no more than the lifetime of temperature displacement from equilibrium which, at high pressure, will be the lifetime of of the shortest lived vibrational state. Also note that both C_v and α_g increase linearly with the pressure in the pressure broadened regime so τ_r will be independent of pressure.

At very low pressures, Eq. (A17) will fail for several reasons. First, we can not then assume that all vibrational modes are in equilibrium with transla-

tion . Second, the gas will become optically thin which will make τ_r pressure dependent. Fortunately, at low pressures, thermal conduction will generally dominate the long term decay and Eq. A17 will represent only a second order effect.

When the pressure is very low collisional processes are comparable in speed to spontaneous emission. As a result, the observed relaxation times will be a combination of collisional, spontaneous emission, and wall deexcitation (discussed later). The combined rate of deexcitation will then be

$$\beta = K_c + K_w + \pi_p$$

Where K_c is the collisional deactivation rate, K_w is the rate of deexcitation by the walls, and π_p is the rate of deactivation by spontaneous emission. There will be a different β for each energy level; for a multi-level system, Eq.(18) is only useful if π_p were the same for each level (it is not).

To a first approximation, we can identify the relaxation times which result from the general reaction matrix (see Eq. A2) with specific levels. For example, the relaxation process which contribures most to sound absorption is associated, to a large extent, with the lower vibrational energy state (assuming series relaxation). The relaxation process which contributes most to fluorescence decay is associated, to a large extent, with the IR mode which fluoresces. These assignments are not rigorous and, should only be used when considering second order effects.

With this assignment, we will write

$$1/\tau_i^{eff} = 1/\tau_i + 1/\tau_i^{rad}$$

where τ_i is the collisional relaxation time in the absence of spontaneous emission, τ_i^{rad} is the radiative lifetime of the level associated with τ_i. Then we replace

τ_{vs}^{i} in Eq. (A2) with τ_{i}^{eff}. The energy which goes into spontaneous emission does not cause the gas temperatures to change so δ_i is replaced by

$$\delta_i(\tau_i^{eff}/\tau_i).$$

There are a variety of other heat loss mechanisms that will help the gas return to equilibrium on the long time scale. Some of these include heat conduction to the windows and absorption of propagating acoustic modes. The significant factor is that these loss mechanisms will increase as 1/p(heat conduction) or be independent of pressure (acoustic loss upon reflection) so they can be included in τ_{tc} or τ_r as appropriate. Our method, then, will be to modify τ_{tc} as necessary to give the correct long term decay at low pressure, and τ_r to give the proper long term decay at high pressures. These second order corrections should provide only third order effects on the more rapid part of the waveform at intermediate pressures.

Appendix B

Effect of Wall Collisions

According to Margottin-Machou, Dogonette, and Henry,[5] the measured relaxation rate $\beta(= 1/\tau_{exp})$ can be written as

$$\beta = K_c + K_w + \pi_p \qquad \text{B1}$$

where K is the collisional deactivation rate, K_w is the rate of deexcitation by the walls, and π_p is the rate of deactivation by spontaneous emission (including trapping). They further show that for a long narrow tube,

$$K_w = \mu^2(D/R^2) \qquad \text{B2}$$

where D is the diffusion coefficient, R is the cell radius and μ is a solution of

$$\mu J^1(\mu) = hJ_o(\mu)$$

where

$$h = (R\bar{\nu}/2D)(a/2 - a)$$

where $\bar{\nu}$ is the mean speed of molecules, and a is the probability of de-excitation during a collision with the cell walls ($\sim$0.4 for CO_2). The ratio R/h is the minimum distance a molecule must travel close to a wall before being deexcited $\gtrsim \lambda/a$ where λ is the main free path. The diffusion coefficient D is pressure dependent so we will write $D_o = DP$.

Margottin-Machou, Dogonette, and Henry found that for pressures of 1 torr and above, μ approaches a limiting value of 2.4 so Eq. B2 becomes

$$K_w = (2.4)^2 D_o / R^2 p \qquad \text{B3}$$

where D_o is the kinetic self-diffusion coefficient.

The interesting feature of the derivation leading to Eq. B3 is the fact that all excited states are deexcited during wall collisions with about the same probability so we can write (ignore spontaneous emission)

$$1/\tau^i_{exp} = 1/\tau^i_{coll} + K_w$$

where the i denotes different relaxation processes. We can, therefore, substitute into Eq. A12 $1/\tau^i_{exp}$ wherever $1/\tau_i$ appears and correct for the change in τ_i resulting from wall collisions. For the spectrophone, however, a change in τ_i is not the only effect on the response. That energy transferred to the tube walls will not contribute to the temperature and pressure rise in the cell so the magnitude of the response will change along with the time constant. The energy which is lost to wall collisions is $K_c/(K_c + K_w)$ times the total energy transferred from vibration so $K_c/(K_c + K_w)$ should give the fraction of the total energy which is transferred to translation due to collisional processes. We must, therefore, replace δ_i in Eq. A11 with $\delta_i(K_c/K_c + K_w)$.

Appendix C - Acoustic Effects

There are several purely acoustic effects which will affect the spectrophone response. These include "acoustic transit", excitation of normal modes of the cavity, and propagating waves. We will consider a cylindrical tube as shown in the following diagram.

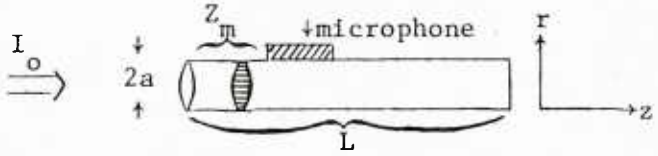

First consider effects of acoustic transit. If the tube is uniformly irradiated in the r direction, the temperature at all radial distances for a given z will evolve together. The transducer only senses pressure increases at r = a but, since the gas is not allowed to expand, this will be the same as the pressure elsewhere along the cross-sections. There will be no radial wave propagation and the microphone will accurately reproduce the pressure response. Uniform excitation is experimentally difficult to achieve. As a worse case, consider a Gaussian excitation with no irradiation near the tube walls. In this case, the center will recieve the greatest energy and a radial pressure wave will move outward impinging upon the transducer a time t = a/C following excitation. One could integrate across the tube cross-section to find the resultant pressure response but such an exercise would only be useful if I(r) was known. It is obvious, however, that for the Gaussian case, the measured pressure will contain information about the kinetics which is an average over events happening on a time scale of a/C. We will call this time the acoustic transit time $\tau_{a.t}$. Note that this represents a worst case. In practice, the beam is probably more nearly uniform than Gaussian so $\tau_{a.t} < a/C$.

There is a second effect of non-uniform excitation across the tube, that is the excitation of radial modes. The cutoff frequency for the first unsymmetric mode is approximately $f_c = 0.586\ C/a$. Radial modes will enhance some components of the pressure response and diminish others. By setting $2\pi f_c = 1/\tau_c$, we can represent the upper frequency response by a time constant τ_c which is the shortest time period for which radial modes will not significantly impact our results. Solving for τ_c,

$$\tau_c = a/1.172\pi C. \qquad \text{C1}$$

which is always less than $\tau_{a.t}$.

The above suggests that for times less than a/C, the uniformity of the excitation beam can begin to have an effect on the measured pressure response. For time segments greater than a/C, acoustic transit and radial modes will not affect the resolution of the experiment. We will choose a such that $\tau_{a.t}$ is always smaller than the resolution desired. The alternative would be to insure a uniform beam cross-section out to the tube walls.

As the laser beam propagates down the tube it will be absorbed in accordance with Beer's Law,

$$I = I_o e^{-\alpha z}, \qquad \text{C2}$$

where α is an extinction length. There is no way, experimentally, to remove this Z dependence of excitation. We can force $\alpha \to 0$ by adjusting the laser frequency and/or gas pressure but this reduces the observed signal proportionately (to first order).

As a result of the exponential illumination, more energy will be absorbed near the entrance window giving a greater pressure rise there than elsewhere down the tube. This difference in pressure rise down the tube will cause a pressure wave propagating down the tube so that the signal received at the microphone will be a sum of signals. Further, if

the tube is terminated at the opposite end, this pressure wave will bounce off the opposite end and set up standing waves. These standing waves can, however, be effectively eliminated by making the tube long enough so that L/C is much longer than the time of interest for studying kinetics. Alternatively, an absorber could be placed at the exit end of the tube.

Assuming all pressure changes are small so that disturbance propagates with the speed of sound, the pressure received at any point z will be

$$p(t,z) = \int_o^z \frac{\partial p(t',z')dz'}{\partial z'} \qquad C3$$

where $t' = t - (z - z')/C$ is the retarded time. Since $p(t',z')$ is directly proportional to the energy absorbed (proportionality constant is time dependent but not z dependent), $\partial p(t',z')/\partial z' = f(t')\alpha I_o e^{-\alpha z'}$ so

$$p(t,z) = \alpha I_o \int_o^z f(t')e^{-\alpha z'}dz'. \qquad C4$$

Further, since the microphone has a finite length, ℓ, along z, the pressure must be averaged along the microphone length so

$$p(t) = \frac{1}{\ell}\int_{z_m}^{z_m + \ell} p(t,z)dz \qquad C5$$

Equations C4 and C5 can be integrated to give p(t) or, z_m and ℓ can be selected to minimize z dependence. This latter requires that $z_m \to 0$ and $\ell \sim \tau_{a.t}\, C$. The first constraint is readily met, the second is not since a very small microphone will reduce sensitivity.

Appendix D

Response of Microphone and Electronics

In addition to thermal conduction, energy transfer to the walls of the cell, and acoustic resonances of the cavity, the response of the microphone and electronics can affect the recorded pressure response. The microphone response, at low frequencies, is determined by leakage of air from front to back of the diaphragm. At high frequencies, the diaphragm begins to oscillate in a resonant mode. The frequency response of the electronics can be controlled by equipment selection and variable frequency filters. It may be more convenient to control the upper and lower frequency cutoffs with filters of known frequency response rather than to rely on theoretical predictions of the frequency response of individual elements. This is especially truewhen the microphone or other components might introduce frequency dependent phase shifts.

The voltage output of a simple capacitor microphone can be written as

$$v(t) = M(p_c - p_b) \qquad \text{D1}$$

where $v(t)$ is the time varying output of the microphone, p_c is the pressure in the cavity, p_b is the pressure behind the diaphragm and M is a sensitivity coefficient which should be independent of frequency at frequencies well below the microphone resonance. The pressure behind the diaphragm will equilibrate with the front pressure with some time constant τ_m dictated by the resistance to air flow front to back. We can write, then

$$dp_b/dt = (p_c - p_b)/\tau_m \qquad \text{D2}$$

and rewrite Eq. D1 as

$$\frac{d}{dt}(p_c - v/M) = v/M\tau_m \qquad D3$$

or

$$\frac{dv}{dt} + \frac{v}{\tau_m} = M\, dp_c/dt. \qquad D4$$

The function $p_c(t)$, the pressure response, can be determined from the preceeding theory. M is just a constant which can be determined (if desired) from microphone calibration curves. We will write the quantity $M\, dp_c/dt = f(t)$, then

$$v(t) = e^{-t/\tau_m} \int_o^t f(t') e^{t'/\tau_m} dt'. \qquad D5$$

Next, we can envision applying this signal to the input of our electronics. The following circuit diagram represents this situation.

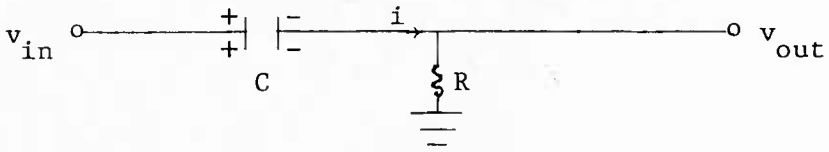

The values of C and R are taken from manufacturers specifications. The equation for voltage becomes

$$v_{in} = q/C + Ri \qquad D6$$

where q is the charge on the input capacitor and i is the current. Recognizing that $i = dq/dt = v_{out}/R$, D6 becomes

$$dv_{in}/dt = 1/C\ (v_{out}/R) + dv_{out}/dt \qquad D6$$

or

$$dv_{in}/dt = dv_{out}/dt + v_{out}/\tau_e, \qquad D7$$

where $\tau_e = RC$.

Combining Eqs. D4 and D7,

$$\frac{dv_{out}}{dt} + v_{out}/\tau_e + v_{in}/\tau_m = M\, dp_c/dt \qquad D8$$

Note that if $\tau_e << \tau_m$, a condition which can be readily controlled experimentally,

$$\frac{dv_{out}}{dt} + 1/\tau_e\, v_{out} \tilde{=} M\, dp_c/dt = f(t) \qquad D9$$

which has a solution

$$v_{out}(t) = e^{-t/\tau_e} \int_o^t f(t')e^{t'/\tau_e}dt'. \qquad D10$$

Ignoring the effect of acoustic modes, $f(t) = \theta(t)$ from Eq. A12 so

$$v_{out}(t) = e^{-t/\tau_e} \int_o^t \sum_{n,i} \Delta_{in} e^{-t'/\tau^n_{tc}}(e^{-t'(1/\tau_i - 1/\tau^n_{tc})} - 1)e^{+t'/\tau_e}dt'. \qquad D11$$

Integrating, D11 becomes

$$v_{out}(t) = e^{-t/\tau_e} \sum_{n,i} \Delta_{in} [(\frac{\tau_i - \tau_e}{\tau_e - \tau_i})(1 - e^{-t(1/\tau_i - 1/\tau_e)}) +$$

$$(\frac{\tau^n_{tc}\tau_e}{\tau_e - \tau^n_{tc}})(1 - e^{-t(1/\tau^n_{tc} - 1/\tau_e)})]. \qquad D12$$

Now, if $\tau_e << \tau_{tc}$, the second term becomes $-\ _e(1 - e^{t/\tau_e})$ and the effects of thermal conduction are effectively filtered out. Although we can typically meet the approximation necessary for D9, at low pressures ($\sim$ 10 torr) $\tau_{tc} \approx \tau_i$ so to make $\tau_e << \tau_{tc}$ would make $\tau_e << \tau_i$ which would eliminate τ_i from Eq. D12; all kinetic information would be lost. At higher pressures, $\tau_e << \tau_{tc}$ is a reasonable approximation.

References

1. Hans - Jörg Bauer, J. Chem. Phys. 57, 3130-3145 (1972).

2. H.S. Carslaw and J.C. Jaeger, "Conduction of Heat in Solids," 188-193 (Oxford University Press, London, 1959).

3. J.M. Weulersse and R. Genier, Appl. Phys. 24, 363-368 (1981).

4. John H. Lienhard, "A Heat Transfer Textbook," 475-480 (Prentice-Hall, Inc., Englewood Cliffs, NJ, 1981).

5. M. Margottin-Maclou, L. Doyenette, and L. Henry, Applied Optics 10, 1768-1780 (1971).

APPENDIX I-C

Pulse Density Modulation of Light for Optical Generation of Sound

by

Henry E. Bass

Sound can be generated at a surface, in a gas, or in a fluid when optical energy is converted to a pressure rise. The mechanism for this conversion can take several forms (thermoelastic expansion, dissociation, vaporization, etc.) but we will be interested, primarily, in thermal expansion which is dominant in a liquid. The thermal expansion mechanism gives a pressure rise which is proportional to $\frac{1}{V}\,(\partial V/\partial T)_s$. The $\frac{1}{V}$ term gives rise to a 1/T term where T is the pulse duration. The 1/T dependence leads us to conclude that maximum sound will be generated by a series of short pulses. If we are to make the resultant meaningful, these pulses must be spaced in occurance, with minimum length, and an amplitude such that an audible signal is produced. We could amplitude modulate a string of pulses to achieve this goal but, from a practical point, it is much easier to modulate the rate of pulses than it is their amplitude. For that reason, we have chosen to examine, in detail, pulse density modulation. Pulse density modulation spaces a sequence of pulses with a time between pulses proportional to the input signal amplitude (to some power).

If we assume a rectangular pulse, we can control the time between pulses and pulse length. We want to produce an acoustic output which will be a true representation of the input electrical signal but it is not obvious how one can best accomplish this objective. For discussion purposes, let us assume that we wish to reproduce a sine wave. Further, as a starting point, we will assume that the optimum output is obtained when the number of pulses/unit time is proportional to the input signal amplitude at that same point in time, i.e.,

$$Np\ (t) = C\ V(t), \qquad (1)$$

where Np(t) is the number of pulses/unit time, and V(t) is the input waveform. Eq. (1) is predicted on the assumption that the output waveform will vary linearly with energy input to the surface provided the input to the surface consists of a number of pulses of the same length.

For a sine wave output, $V(t) = \sin \omega t$, so

$$Np(t) = C \sin \omega t. \tag{2}$$

The number of the pulse can never be negative so we must modulate about some average number of pulses, A,

$$Np(t) = \frac{A}{2} (a + b \sin \omega t). \tag{3}$$

Note that although $a + b = 2$, the ratio a/b controls the degree of modulation. With $a/b = 1$, there are no pulses emitted when V(t) has its most negative value; when $a/b = 0$, there is no modualtion. We will require that $a \geq b$ so the term in parenthesis will not go negative.

Expressed in terms of the time between pulses, t_b,

$$t_b = \frac{2}{A} (a + b \sin \omega t)^{-1}. \tag{4}$$

Let P_r = maximum pulse repetition frequency, then

$$t_b = \frac{4}{Pr} (a + b \sin \omega t)^{-1} \tag{5}$$

if we want a maximum duty cycle of 50%. If we want a smaller duty cycle, f_d,

$$t_b(t) = a/[f_d P_r (a + b \sin \omega t)] \tag{6}$$

where f_d is the maximum fraction of time the light source is on.

In order to examine the waveform generated by a series of pulses spaced in time according to Eq (6), a numerical simulation was employed. We examined one cycle of a 100 Hz sine wave ($V(t) = \sin 2\pi ft$). We further assumed that the pulse duration was 10 μsec or 10^{-3} cycles (actually, we used 1024 to simplify the Fourier Transform). We then place a 1 or a 0 in a 1024 point array to indicate a pulse on or off. We did this by evaluating Equation (6) and determining if the time since the last 1 was greater than or equal to $t_b(t)$ for each 10 μ sec interval of time. This array was then transformed into the frequency domain to determine the resultant waveform.

There were two features of the frequency domain spectrum of interest; the signal to noise ratio and the fraction of energy appearing at the desired frequency (100 Hz). We took the signal to noise ratio to be $20 \log_{10}[A(100Hz)/A(200Hz)]$ where A(f) is the amplitude of the Fourier Transform at a frequency f. We took to conversion efficiency (CE) to be $20 \log_{10}[A(100Hz)/A(DC)]$ since most energy lost to the 100Hz signal appeared in the DC term.

The first set of results (Figure 1) are for a pulse length of 1/6400 sec. It can be seen that the S/N ratio is reasonably constant for b/a $\sim$ 0.5 to 1.0 but it has a low value $\sim$ 10 dB. The conversion is also given for a pulse length of 1/12,800 sec; the S/N is better, the CE is worse. Note that for these figures, the duty cycle has a maximum of 50%.

The next results (Figure 2) are for a pulse length of 10 μsec but variable duty cycle fraction. First, looking at the S/N, we see that, with the exception of some peaks, the S/N varies directly with PRF from about 22dB for a PRF of 6400 Hz (64 x the fundamental frequency) to $\sim$ 10dB for a PRF of 1600 Hz (16 x the fundamental frequency). The conversion efficiency does not change much in this PRF range; it drops uniformly with the b/a ratio (at b/a = 0, CE = 0). The plots of S/N do illustrate that optimum S/N occurs for b/a < 1.0. This means that when the signal swings negative, the number of pulses/sec emitted by the light source never goes to zero. The optimum swing in signal (b/a) is dependent on PRF; it decreases as the PRF increases.

The above results suggest that PDM will be effective (acceptable S/N) only if the pulse length is short and the PRF is high. Considering light sources off the shelf, this argues for a fast Xenon flash lamp or a laser diode system. A typical off the shelf Xenon flashtube emits a maximum energy/flash of 15 joules in < 15 μsec at a maximum of 2500 pps. A laser diode system will emit an average of 6 m watts with a pulse length less than 10 nanoseconds at 100 M pps.

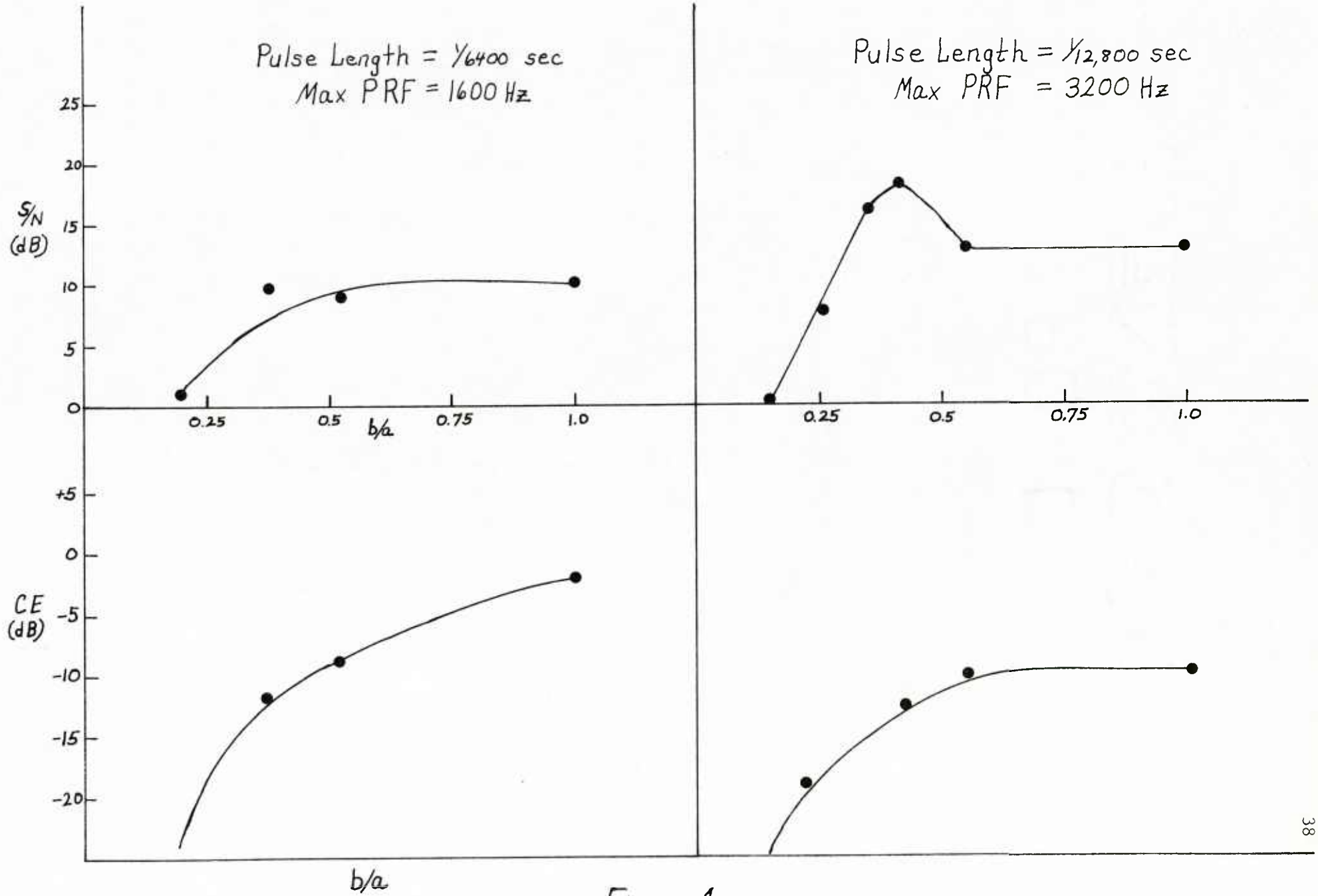
Pulse Length = 1/6400 sec
Max PRF = 1600 Hz
Pulse Length = 1/12,800 sec
Max PRF = 3200 Hz
S/N (dB)
25
20
15
10
5
0
0.25
0.5
0.75
1.0
b/a
+5
0
-5
-10
-15
-20
CE (dB)
b/a

Figure 1

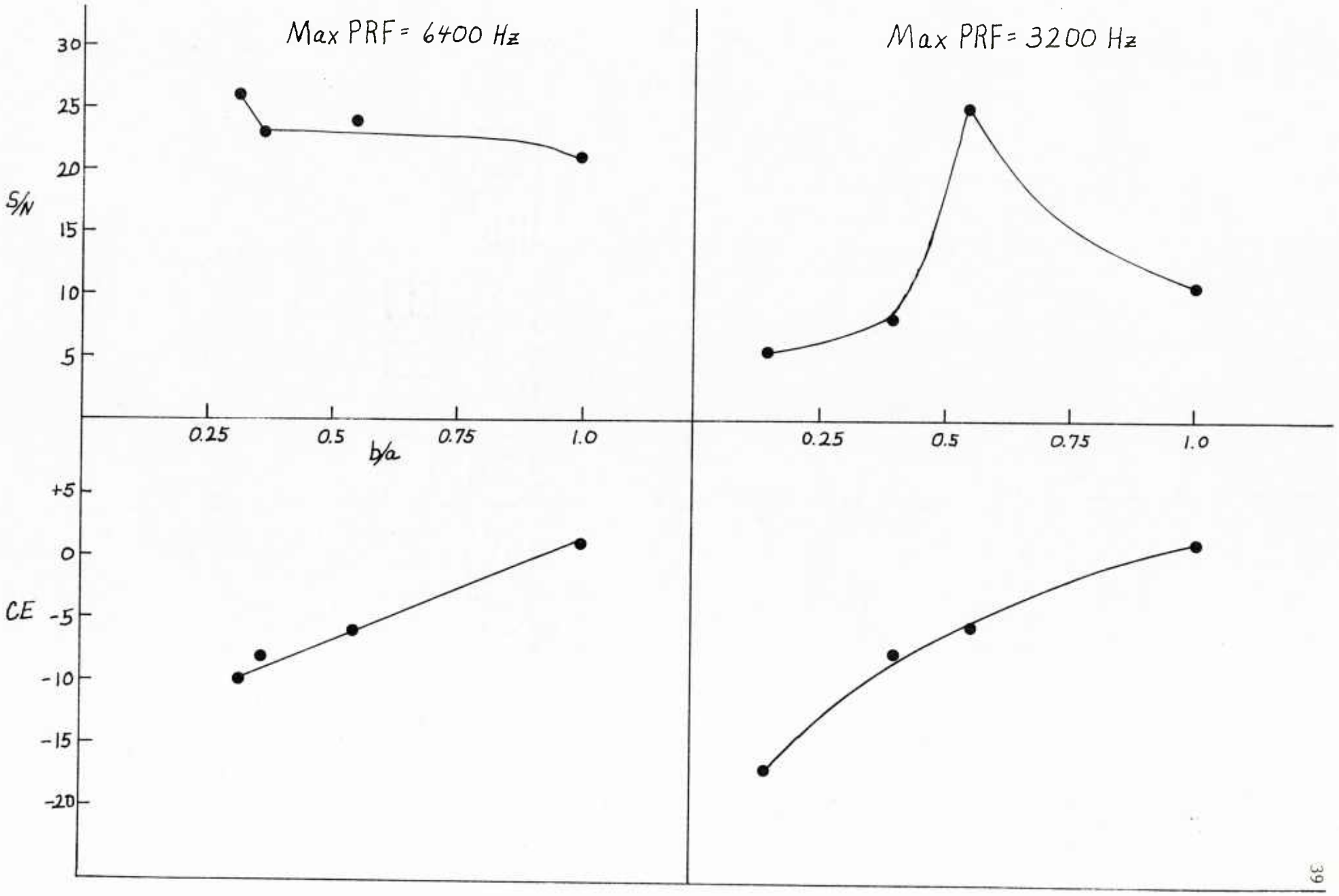
Max PRF = 6400 Hz
Max PRF = 3200 Hz
S/N
30
25
20
15
10
5
0.25
0.5
0.75
1.0
b/a
CE
+5
0
-5
-10
-15
-20

2a.

2b.

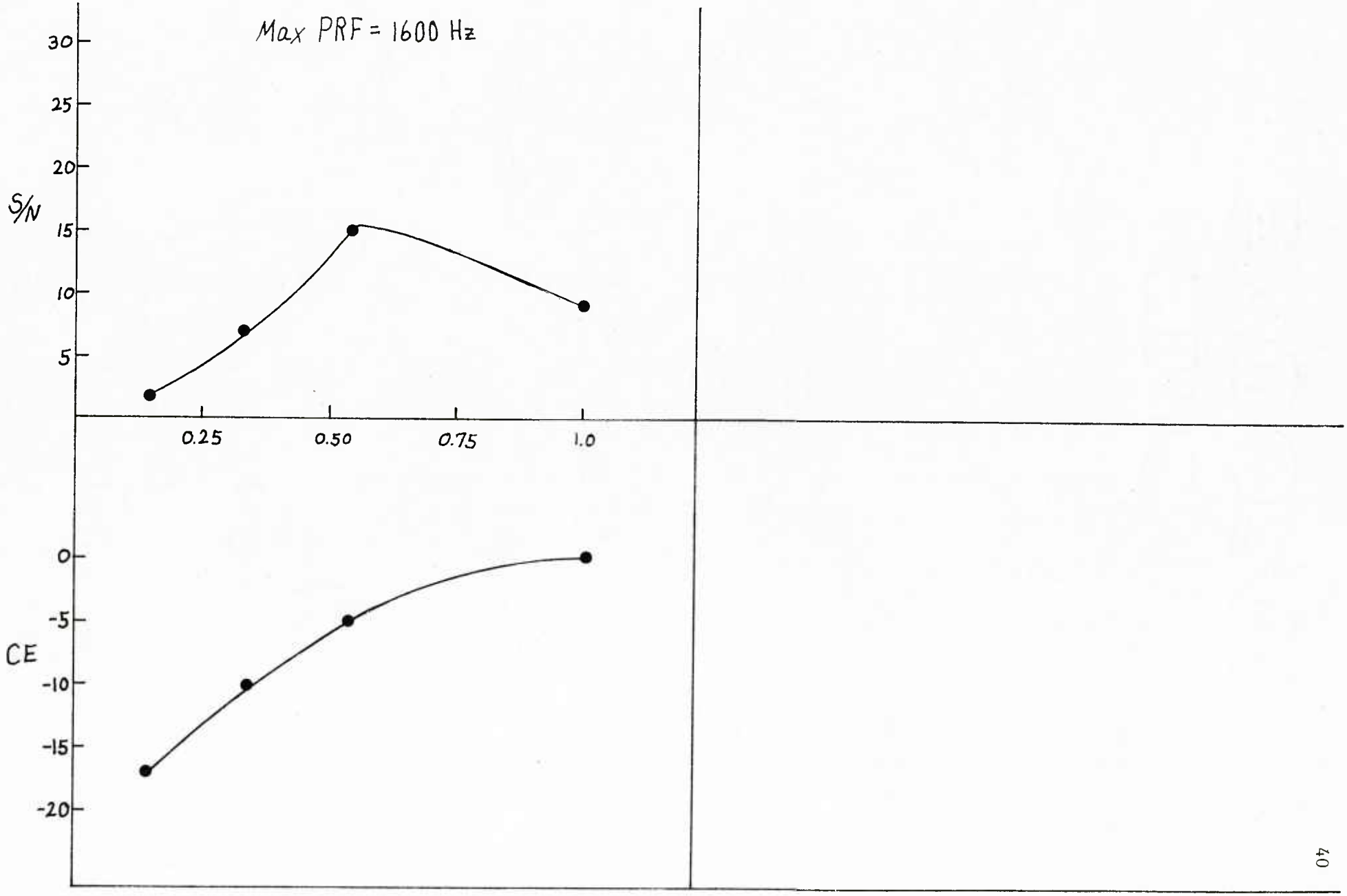

2c.

Task II

This task involves the generation of acoustic waves from the interaction of a modulated CO_2 laser pulse with a highly absorbing liquid medium such as water. Earlier experiments in water with proton beams [Hunter et. al., J. Acoust. Soc. Am. 69, 1557-1562 (1981)] and with laser pulses [Hunter, Jones and Malbrough, J. Acoust. Soc. Am. 69, 1563-1567 (1981)] gave both dipolar and tripolar signals that did not vanish at 4°C.

Since these pulses were presumed to be generated by the thermoelastic properties of the liquid, it was not understood why they still existed at 4°C. Recently, Pierce [J. Acoust. Soc. Am. 72, S13 (1982)] has suggested that acoustic signals may be generated at 4°C if one considers the effect of volume relaxation. He has suggested a series of experiments to test these predictions.

We have increased the peak output of our CO_2 laser system with the acquisition of an optical scanner that will enable us to vary the prf from dc to 2 kHz. We hope soon to obtain data on the amplitude of the thermoelastic signal as a function of temperature and a variety of other liquid parameters.

Propagation of Sound through Gases with an Overpopulation of Excited Vibrational States.

Introduction

The propagation of sound through gases under a variety of non-equilibrium conditions has been studied the past ten years. These studies have predicted sound amplification in the presence of a chemical reaction[1-4] or optical pumping of vibrational states[5-7]. Bauer and Bass have named the later process "SACER", which is an acronym for "sound amplification from controlled excitation reactions." The predicted amplification is attributed to the preferential heating of the compression part of the sound wave either by the pumping process or the relaxation process or both. The amplification due to pumping results from the selective absorption of pumping energy in the compression part of the sound cycle. The amplification due to relaxation results from the temperature dependence of the vibrational energy transition rate. The increase in the rate of v-t energy transfer with temperature causes the relaxing vibrational energy to be selectively "dumped" into the hot (or compressional) part of the sound cycle. When the sound wave is propagated in the presence of pumping, both effects are likely to be operative and the two will be difficult to separate. In addition, the non-equilibrium conditions produced by the pumping make accurate measurement of the sound amplification or absorption difficult.

A situation more amenable to experimental study results if the pumping process can be terminated and a metastable state allowed to develop in the gas before the sound wave is introduced. In this case it is obvious that the decay time must be long compared to the sound period. Three typical situations where such a condition could be produced by pumping energy into a particular vibrational mode are:

(1) A single long lived relaxing mode. Most stable diatomic gases fall into this category. Bauer and Bass have considered the case of a mixture of CO and H_2 and predict large amplification when the period of the wave is close to the relaxation time of the excited state[7]. As mentioned above, if the measurements are made after the pumping mechanism is removed, frequencies in this range are ruled out. This study considers the possibility of observing the amplification when the sound has a period that is short compared to the relaxation time.

(2) Fast v-v and slow v-t exchange. For most pure polyatomic gases, and in some gas mixtures, vibrational energy exchanges rapidly between modes by a fast v-v exchange and then more slowly with translation by a slow v-t exchange. It was early recognized that such a "fast series process" would lead to single-relaxation-time sound absorption and dispersion curves and the process was invoked to explain the single-relaxation times observed for most polyatomic gases.[8,9]

If an upper vibrational level of such a gas is pumped, a metastable state with different vibrational modes at different temperatures results. The whole manifold of vibrational states then decays at a slow rate. The resonant v-v exchange within a given mode is still fast compared to v-v exchange between modes. An example of this stiuation is CH_3F.[10,11] The vibrational modes equilibrate on a time scale corresponding to 100 gas kinetic collisions and then the whole system decays together with a relaxation time of the order of 2×10^{-6} sec atm which corresponds to about 1500 gas kinetic collisions.

Sound propagating through a gas in this kind of metastable state could show some interesting effects. Even if the sound frequency is far above the v-t relaxation regions and is not communicating translational energy into and out of vibration by the v-t process, there still may be

communication of translational energy into and out of vibration due to the non-resonant exchange between vibrational modes. To understand this, consider what happens in the compression-rarifaction cycle of the sound wave. When the translational temperature increases upon compression the v-v transition rates change. The number of molecules traveling the endothermic direction of a reaction increases more than the number going the opposite direction with the result that one vibrational mode increases in temperature more than the other. The reverse change takes place in the rarifaction part of the cycle. When the sound frequency is close to the v-v transfer rate, the process transfers energy from the compression to the rarifaction producing sound absorption. When there is an overpopulation of vibrational states, the slowly decaying vibrational states again dump energy selectively in the compression part of the sound cycle, due to the temperature dependence of the transition rates. This reduces the absorption or even causes amplification. Measurement of the effect could give valuable information about relaxation paths, the transition rates, and their temperature dependence.

(3) Slow v-v and fast v-t. In some cases the v-v rate may be slower than the v-t rate. SO_2 is an example of this situation.[12] The v-t rate is about 10 times the v-v rate. In this case, which might be compared to the two step decay of a radioactive isotope, energy pumped into the long-lived mode feeds by v-v transfer a second mode that is communicating with translation by v-t transfer and maintains its vibrational temperature above the equilibrium value for periods comparable to the v-v relaxation time rather than the v-t time. In this case also experimental observation of sound amplification may be possible and measurements may give valuable knowledge about the energy transfer process.

The Reaction Equation

The sound absorption (or amplification) and velocity can be obtained from the imaginary and real parts of the propagation constant for plane waves (k_s). For this purpose we write

$$k_s = \omega\sqrt{\frac{M}{RT}}\sqrt{\frac{C_v}{C_p}}\ , \qquad 1.$$

where ω is the angular frequency, M is molecular weight, R is the gas constant, T is absolute temperature, and C_v and C_p are the specific heat at constant volume and pressure. In the presence of relaxation, C_v and C_p are time dependent or, for a sinusoidal wave, complex and frequency dependent. The sound absorption (α_s) and velocity (v_s) are given by

$$\alpha_s = \text{Imaginary part of } k_s$$

$$v_s = \omega \times [\text{Real part of } k_s]^{-1} \qquad 2.$$

The problem of calculating the sound absorption and velocity is thus reduced to finding the real and imaginary parts of the complex, frequency-dependent specific heats, C_v and C_p.

For this purpose, we begin with the reaction equation which gives the time rate of change of energy in a vibrational mode. We will assume that the normal modes of vibration can be treated as harmonic oscillators and that resonant exchange of energy between the vibrational levels within a single mode rapidly establish a Boltzmann distribution within the mode characterized by a "vibrational temperature".[13,14] In the metastable state here considered, the vibrational temperatures for the different modes may differ from each other and from the translational temperature and will be changing slowly on the time scale of the sound-wave period.

The time rate of change of energy in the $a^{\underline{th}}$ vibrational mode can be written as[15]

$$\dot{E}_a = \sum_{i,j} ih\upsilon_a \mathcal{P} \sum_{\alpha=0}^{\infty} \sum_{\beta=0}^{\infty} \left(k^{\alpha\to\alpha+i,\beta\to\beta+j}(a,b)\ \frac{n_\alpha(a)n_\beta(b)}{N_b}\right.$$
$$\left. -k^{\alpha+i\to\alpha,\beta+j\to\beta}(a,b)\ \frac{n_{\alpha+i}(a)n_{\beta+j}(b)}{N_b}\right). \qquad 3.$$

This equation assumes that mode "a" is exchanging energy with a second mode "b", and with translation. Modes a and b can be in the same molecule or, in the case of a gas mixture, in different molecules. The inclusion of additional modes of interaction is straight forward.[15] α and β refer to the vibrational quantum number of modes a and b, h is Planck's constant, υ_a is the fundamental vibrational frequency of mode a, $\mathcal{P}$ is pressure, N_b is the total number of molecules carrying mode b, n_α and n_β are the number of molecules with α and β quanta in modes a and b, respectively, $k^{\alpha\to\alpha+i,\beta\to\beta+j}(a,b)$ is the composition-averaged rate constant in the dimensions (time x pressure)$^{-1}$ for the particular process in which α changes to $\alpha+i$ and $\beta\to\beta+j$ in the mixture. The summations over α and β gives a net rate constant for transitions where mode a gains i quanta and mode b gains j quanta. In general, only transitions where i and j have different signs are likely to occur, i.e., mode a gains i quanta and mode b loses j quanta or vice versa.

For linear perturbations of harmonic oscillators,

$$k^{\alpha\to\alpha-i,\beta\to\beta+j}(a,b) = \{[\alpha(\alpha-1)\cdots(\alpha-i+1)] \times [(\beta+j)(\beta+j-1)$$
$$\cdots(\beta+1)]/i!j!\} \times k^{i\to o,o\to j}(a,b) \qquad 4.$$

In terms of collision efficiencies, $k^{\alpha\to\alpha+i,\beta\to\beta+j}$ can be written

$$k^{\alpha\to\alpha+i,\beta\to\beta+j} = \Sigma_p x_p M_p P^{\alpha\to\alpha+i,\beta\to\beta+j}(a,b,p), \qquad 5.$$

where $P^{\alpha\to\alpha+i,\beta\to\beta+j}(a,b,p)$ is the collision efficiency for the designated transitions, p denotes the collision partner (if the collision does not allow the transition P = 0), and M_p is the collision rate of a molecule of type a in a gas of type p at unit pressure. $M_p P^{\alpha\to\alpha+i,\beta\to\beta+j}(a,b,p)$ is, therefore, the usual rate constant. x_p is the mole fraction of gas of type p.

We now assume that resonant exchanges of energy between levels of a single mode rapidly establish a Boltzmann distribution of energy within each mode so that we can write

$$n_\alpha = n_o(a)e^{-\alpha h\nu_a/kT_a} = N_a(1-e^{-h\nu_a/kT_a})e^{-\alpha h\nu_a/kT_a}. \qquad 6.$$

Thus, each mode has its own temperature which in the general case is different from the translational temperature. Following conventional notation we set

$$\frac{h\nu_a}{k} = \theta_a, \text{ and } 1-e^{-\theta_a/T} = \chi_a(T). \qquad 7.$$

(Note that this is a change in notation from ref. 15.)

Using equations 4 and 6, the reaction equation (Eq. 3) can be summed over α and β. For this purpose note that

$$\Sigma_\alpha(\alpha+i)(\alpha+i-1)\cdots(\alpha+1)x^\alpha = \frac{d^i}{dx^i}\left(\frac{1}{1-x}\right) = \frac{i!}{(1-x)^{i+1}}$$

After summing over α and β Eq. 3 becomes

$$\dot{E}_a = \sum_{i,j} iN_a h\nu_a \wp[k^{i\to o,o\to j}(a,b)e^{-i\theta_a/T_a} - k^{o\to i,j\to o}(a,b)e^{-j\theta_b/T_b}]/$$
$$[\chi_a(T_a)]^i\,[\chi_b(T_b)]^j. \qquad 8.$$

For a discussion of the case where the modes are degenerate, see ref. 15.

A Single Long-Lived Relaxing Mode

If the vibrational temperatures can be determined, Eq. 8 allows the determination of the sound absorption and velocity in the excited gas. The three cases discussed in the introduction would be delineated by the choice of transition rates. To illustrate, we specialized to the simplest case, that of a gas with a single long-lived relaxing mode. In this case $j = 0$ and $i = 1$. The sum over i and j has only one term and Eq. 8 becomes, after some manipulation,

$$\dot{E}_a = - k^{10}\chi_a(T)[E_a(T_a) - E_a(T)], \qquad 9.$$

where $E_a(T_a) = N_a k\theta_a e^{-\theta_a/T_a}/\chi_a(T_a)$ and $E_a(T) = N_a k\theta_a e^{-\theta_a/T}/\chi_a(T)$. This of course, is the expected relaxation equation with the relaxation time, τ, equal to $[\, k^{10}(\chi_a(T)]^{-1}$.

Now consider the case where a sound wave is propagated through a slowly relaxing gas. Either by differentiating Eq. 9 or by differentiating Eq. 3 and the summing over α and β, we obtain

$$\Delta\dot{E}_a = \dot{E}_a^o \{ [\frac{1}{p}\frac{dp}{dT} + \frac{1}{k^{10}}\frac{dk^{10}}{dT} - \frac{\theta_a e^{-\theta_a/T}}{T^2\chi_a(T)}]\Delta T - \frac{\Delta E_a(T_a) - \Delta E_a(T)}{\tau \dot{E}_a^o}\}. \qquad 10.$$

Here we make use of the fact that the transition rate is a function of translational temperature only and we neglect higher order terms in the sound variables. E_a^o, T_a and T now represent unperturbed values, i.e., values without the sound wave. Introducing the sinusoidal time dependence and setting $\Delta E_a(T_a) = C_a(T_a)\Delta T_a$, $\Delta E_a(T) = C_a(T)\Delta T$, and $\dot{E}_a^o = -\frac{E_a(T_a)-E_a(T)}{\tau}$, this equation becomes

$$(1+j\omega\tau)\frac{\Delta T_a}{\Delta T} = [\frac{\dot{E}_a^o\tau}{C_a(T_a)}] \times [\frac{1}{p}\frac{dp}{dT} + \frac{1}{k^{10}}\frac{dk^{10}(a)}{dT} - \frac{\theta_a e^{-\theta_a/T}}{T^2\chi_a(T)}] + \frac{C_a(T)}{C_a(T_a)}. \qquad 11.$$

In this form it is easy to see the effect of the overpopulation of excited states on the usual absorption due to relaxation. In the "usual case", that is when the gas has not been "pumped", $\dot{E}_a^o = 0$, and $T_a = T$, and the right hand side of Eq. 5 is unity. Then $\Delta T_a/\Delta T = (1+j\omega\tau)^{-1}$. Writing the frequency independent part of the specific heat as C_∞, the frequency dependent specific heats become

$$C_v(\omega) = C_\infty + C_a\Delta T_a/\Delta T = C_\infty + C_a(1+j\omega\tau)^{-1} \qquad 12.$$

and

$$C_p(\omega) = C_v(\omega) + R \qquad 13.$$

The familiar absorption and velocity versus frequency curves are those corresponding to a single-relaxation-time process.

When $T_a \neq T$, $\dot{E}_a^o \neq 0$ and the frequency dependent specific heats are

$$C_v(\omega) = C_\infty + C_a'/(1+j\omega\tau) \qquad 14.$$

$$\text{with } C_a' = \dot{E}_a^o\tau\left[\frac{1}{T} + d[\ln k_{10}(a)]/dT - \frac{\theta_a e^{-\theta_a/T}}{T^2\chi_a(T)}\right] + C_a(T) \qquad 15.$$

and

$$C_p(\omega) = C_v(\omega) + R - \frac{\dot{E}_a^o\tau}{T(1+j\omega\tau)}. \qquad 16.$$

Here R is the universal gas constant and $\frac{1}{p}\frac{dp}{dT}$ has been given its ideal gas value of $\frac{1}{T}$. The extra term in C_p results from the fact that, at constant pressure, $\partial p/\partial T = 0$.

It is possible, therefore, to plot $C_p(\omega)$ and $C_v(\omega)$ as $\omega \to 0$, and the sound absorption and dispersion in a particular gas as a function of the decay rate, $\dot{E}_a^o$. Bauer and Bass have done this for a CO/H_2 mixture, treating the CO as having two vibrational states. If $\dot{E}_a^o$ is set equal to the negative of their pumping rate, the two treatments give similar results.

For the purposes considered here, it is more useful to set

$$\dot{E}_a^o = -\tau^{-1}[E_a(T_a) - E_a(T)] \qquad 17.$$

and express the results in terms of the vibrational temperature T_a. Sound amplification will occur when C_a' becomes negative. (Note that $\dot{E}_a^o$ is negative.) We now seek to determine values of T_a needed to produce this sound amplification, the magnitude of the amplification, and the experimental conditions under which it can be observed.

Calculation and Observation of the Sound Amplification

For most diatomic gases, (the halogens would be an exception), the relaxation time is so long in the pure gas that collisions with impurity molecules usually control the relaxation process. For such collisions, $\frac{d(\ln k_{10})}{dT}$ is of the order of a few one hundreds[16] and amplification will occur when T_a-T is a few tens of degrees.

However, observing this amplification in a metastable state in the absence of pumping is difficult. For frequencies where the sound period is short compared to the relaxation time (a requirement for the metastable state to persist over a number of sound vibrations), $\omega\tau$ will be large and the gain per unit length of sound path will be small. Furthermore, the length of the sound path is restricted since the transit time for the sound wave through the gas must be small compared to the relaxation time.

In the case of polyatomic gases with molecular dipole moments and correspondingly high optical absorption coefficients, it may be possible to extend the sound path length by pumping the gas ahead of a sound pulse with a laser beam swept through the gas. However, such a configuration does not appear practical for the diatomic case here considered. In the first place to absorb the laser light the diatomic gas would need a molecular dipole moment and in addition the long relaxation times would require large volumes and hence large power.

This means that high vibrational temperatures are needed to produce observable amplification of the sound in the diatomic case. Table 1 gives values of the gain in db/wavelength for some typical diatomic gases as calculated from Eqs. 1,2,9,10 and 11. In these calculations $\omega\tau$ is set equal 100 and, in this range, the gain is approximately inversely proportional to $\omega\tau$. However, values much smaller than 100 violate the metastable state requirement since at this value τ corresponds to approximately 16 sound periods. The value of $\frac{d}{dT} \ln k_{10}$ has been taken to be 0.01, which, as mentioned above, seems to be representative.

Table I. Sound amplification in db per wavelength for typical diatomic gases at 300° K with elevated vibrational temperatures, T_a. The derivative of the natural logarithm of the transition rate, $d(\ln k_{10})/dT$, has been set equal to 0.01. The amplification is approximately inversely proportional to $\omega\tau$.

gas	$\nu(cm^1)$	Amplification (db/λ) with $\omega\tau$ = 100					
		T_a = 400°K	600°K	1000°K	1500°K	2000°K	4000°K
N_2	2331	8.6×10^{-4}	0.016	0.16	0.54	1.0	3.4
CO	2143	1.5×10^{-3}	0.024	0.20	0.61	1.1	3.6
O_2	1556	7.5×10^{-3}	0.071	0.36	0.87	1.5	4.0
Cl_2	557	5.0×10^{-2}	0.26	0.74	1.4	2.0	4.6

References

1. R.G. Gilbert, H.S. Halin, P.J. Ortoleva, and J. Ross, J. Chem. Phys. 57, 2672 (1972).

2. R. Gilbert, P. Ortoleva, and Jolen Ross, J. Chem. Phys. 58, 3624 (1973).

3. Jean-Pierre Patureau, Tau-Yi Toong and Charles A. Gavis, 16th International Symposium on Combustion, Mass. Inst. of Tech., Boston, Mass., 1976, p. 929.

4. Robert J. Ellis, and Robert G. Gilbert, J. Acoust. Soc. Am. 62, 245 (1977).

5. E.P. DePlomb, Phys. Fluids 14, 488 (1971).

6. Michael Schulz, Phys. Fluids 11, 676 (1968).

7. H.J. Bauer and H.E. Bass, Phys. Fluids 16, 988 (1973).

8. K. Schafer, Z. Physik Chem. B46, 212 (1940).

9. F. Douglas Shields, J. Acoust. Soc. Am. 47, 1262 (1970).

10. I. Shamah, and G. Flynn, J. Chem. Phys. 69, 2475 (1978).

11. E. Wietz and G. Flynn, Advances in Chem. Phys. vol. XLVII, Photo-Selective Chemistry, Part II, Ed. Joshua Jortner, Rapheal D. Levine, and Stuart A. Rice, John Wiley & Sons, New York, 1981.

12. F. Douglas Shields, J. Chem. Phys. 46, 1063 (1957). F.D. Shields and B. Anderson, J. Chem. Phys. 55, 2636 (1971). B. Anderson and F.D. Shields, J. Chem. Phys. 56, 1147 (1972).

13. C.E. Treavor, J.W. Rich, and R.G. Rehm. J. Chem. Phys. 48, 1798 (1968).

14. W.D. Breshears, and L.S. Blair, J. Chem. Phys. 59, 5824 (1973).

15. H.J. Bauer, F. Douglas Shields, and H.E. Bass, J. Chem. Phys. 57, 4624 (1972).

16. R.L. Taylor and S. Bitterman, Rev. Mod. Phys. 41, 26 (1969).

Task IV

This task involves general studies in acoustic cavitation. We have made progress along four lines:

1. In a study of the nonlinear oscillations of individual gas bubbles that are acoustically levitated in a liquid, we have been able to measure (a) the polytropic exponent of the gas contained within the interior of the bubble, and (b) certain aspects of the pulsation amplitude relating to excitation of the second harmonic resonance of the bubble oscillation. Two papers describing the results of this particular study are scheduled for publication in early 1983 in the Journal of the Acoustical Society of America. Some of this work has been done in collaboration with Audrea Prosperetti of the University of Milan, Italy. Abstracts of these papers are included As Appendix IV-A and IV-B.

2. Previously, the equations that describe the growth of air bubbles by rectified diffusion have been done mostly in a piecemeal fashion. We have generalized these equations by extending their range of applicability. A paper describing this work has appeared in the November issue of the Journal of the Acoustical Society of America. This abstract is included as appendix IV-C.

3. We have examined the effect of dilute polymer additives on the acoustic cavitation threshold of water. We discovered that the addition of very small amounts of these additives <u>increase</u> the cavitation threshold - a desirable effect. Our explanation for why this occurs involves the way the reduced liquid surface tension (the additives are surface-active) affect the nucleation conditions. A paper describing the results of this study has been submitted for publication in the Journal of Fluids Engineering.

The abstract of this paper is included as appendix IV-D.

4. A tremendous amount of interest has recently been generated by certain suggestions that ultrasonic scanners used as diagnostic devices may cause transient cavitation. A recent paper by Flynn [J. Acoust. Soc. Am. 72, 1926-1932 (1982)] has predicted the presence of acoustic cavitation by these devices. We have attempted to verify this prediction experimentally. We have found that cavitation can be produced by single acoustic pulses; however, our pulses have been at high kilohertz frequencies rather than the megahertz frequencies associated with most diagnostic scanners. We are redesigning our apparatus to examine these higher frequencies. A report of our active work in this area was recently given at the Bureau of Radiological Health; an abstract of that presentation is included as appendix IV-E.

Further, a general review article on acoustic cavitation was presented at the IEEE International Symposium on Sonics and Ultrasonics. This review paper will be published in the proceedings of that symposium. An abstract of that presentation is included as appendix IV-F.

Appendix IV-A

The Polytropic Exponent of Gas Contained Within Air Bubbles Pulsating in a Liquid. Lawrence A. Crum, Physical Acoustics Research Laboratory, Department of Physics, University of Mississippi, Oxford, MS 38677

Gas bubbles that are driven into oscillation within a liquid pulsate with amplitudes that are determined largely by the thermodynamic behavior of the gas contained within the bubble. Theoretical approaches to the solution of the motion of the radius of the bubble normally involve the polytropic exponent of the gas. Measurements are presented of this exponent for three different gases and for a wide range of values of the exponent. Comparison with available theories indicates good agreement between measurements and predictions provided the gas bubble is not driven near one of its harmonic resonances.

To be published in the Journal of the Acoustical Society of America, early, 1983.

Appendix IV-B

Nonlinear Oscillations of Gas Bubbles in Liquids: An Interpretation of Some Experimental Results. Lawrence A. Crum, Physical Acoustics Research Laboratory, Department of Physics, University of Mississippi, Oxford, MS 38677 and Andrea Prosperetti, Istituto di Fisica, Universita di Milano, Italy.

Measurements are presented in this paper of the pulsation amplitude of an individual air bubble that is levitated in a glycerine-water mixture by a stationary acoustic wave operating at a frequency of 22.2 kHz. Observations of the bubble pulsation for a wide range of bubble sizes demonstrate the existence of the n = 2 harmonic resonance ($\omega \simeq \omega_o/2$). The available theoretical information on linear and nonlinear bubble oscillations is adapted to apply to the specific experimental conditions. Comparisons made with the theory show excellent agreement between measurements and predictions.

To be published in the Journal of the Acoustical Society of America, early 1983.

Appendix IV-C

Generalized Equations for Rectified Diffusion. Lawrence A. Crum and Gary M. Hansen, Department of Physics and Astronomy, University of Mississippi, Oxford, MS 38677

There are at least four different equations present in the literature for the threshold for growth of gas bubbles by rectified diffusion. These various equations have limited regions of applicability and also give significantly different predictions in common regions of applicability. In this paper, a set of general equations are obtained for the growth rate and the threshold for rectified diffusion that apply over a wider range of interest. It is shown that under certain restrictions the previous equations agree with the more general ones given here. Finally, graphical representations of the equations are given showing the degree of approximation and the range of applicability of the specialized equations.

Published in the November, 1982, issue of the Journal of the Acoustical Society of America.

Appendix IV-D

Effect of Dilute Polymer Additives on the Acoustic Cavitation Threshold of Water

Lawrence A. Crum
Professor of Physics

and

James E. Brosey
Graduate Assistant

Department of Physics
University of Mississippi
Oxford, MS 38677

ABSTRACT

Measurements are presented of the variation of the acoustic cavitation threshold of water with concentration of the polymer additives polyethylene oxide and guar gum. It was found that small amounts of these additives could significantly increase the cavitation threshold. A theoretical model, based upon nucleation of a gas bubble from a Harvey-type crevice in a mote or solid particle, is developed that gives good agreement with the measurements. The applicability of this approach to an explanation of cavitation index reduction in flow-generated or confined jet cavitation, when polymer additives are introduced, is discussed.

Submitted for publication in the Journal of Fluids Engineering.

Appendix IV-E

Acoustic Cavitation and Some Possible Biophysical Effects

Various aspects of acoustic cavitation will be discussed and movies will be shown of the different types of cavitation observed in a liquid. Recent observations of cavitation effects in tissue will be described as well as some possible explanations for these effects in terms of bubble growth by rectified diffusion and transient cavitation inception. Finally, some recent work on the cavitation produced by microsecond-length pulses will be discussed.

Presented at the Food and Drug Administration National Center for Devices and Radiological Health, Thursday, December 9, 1982.

Appendix IV-F

ACOUSTIC CAVITATION IN LIQUIDS*

LAWRENCE A. CRUM, Physical Acoustics Research Group, Department of Physics, University of Mississippi, Oxford, MS 38677.

A broad review will be given of the phenomenon of acoustic cavitation, generally defined as any observable activity involving a bubble or population of bubbles stimulated into motion by an acoustic field. Discussions will be given of cavitation inception - thresholds, nucleation, tensile strength of liquids; bubble dynamics - rectified diffusion, nonlinear oscillations, cavity collapse; and cavitation effects - sound attenuation, material erosion and biological damage. Movies depicting various aspects of cavitation phenomena will be shown.

*This work has been supported in part by ONR, NSF and NATO.

L. A. Crum
Physical Acoustics Research Group
Department of Physics & Astronomy
The University of Mississippi
Oxford, MS 38655
(601) 232-5840

To be published in the Proceedings of the IEEE Symposium on Sonics and Ultrasonics.

Task V

This task involves the acoustic measurement of energy and momentum accomodation coefficients. Under this task, an acoustic technique is used to determine these coefficients. A technical report was distributed. The abstract of this report is included as Appendix V-A.

Appendix V-A

Abstract for technical report submitted October 20, 1982. This report will be published as a paper in the Journal of Chemical Physics in early 1983.

ABSTRACT

Acoustical measurements of energy and tangential momentum accomodation coefficients indicate stable and reproducible Pt and Ag surfaces are obtained by heating in a vacuum. EAC and TMAC values are given for He and Ne on the heat-cleaned Pt and Ag surfaces and for these gases on Pt and Ag surfaces after exposure to various adsorbent gases. AC values are also given for the various adsorbent gases on themselves on the heat-cleaned Pt and Ag surfaces.

DISTRIBUTION LIST

Director Defense Advanced Research Projects Agency Attn: Technical Library 1400 Wilson Blvd. Arlington, Virginia 22209	3 copies
Office of Naval Research Physics Program Office (Code 421) 800 North Quincy Street Arlington, Virginia 22217	3 copies
Office of Naval Research Director, Technology 800 North Quincy Street Arlington, Virginia 22217	1 copy
Naval Research Laboratory Department of the Navy Attn: Technical Library Washington, D.C. 20375	3 copies
Office of the Director of Defense Research and Engineering Information Office Library Branch The Pentagon Washington, D.C. 20301	3 copies
U.S. Army Research Office Box 12211 Research Triangle Park North Carolina 27709	2 copies
Defense Technical Information Center Cameron Station Alexandria, Virginia 22314	12 copies
Director, National Bureau of Standards Attn: Technical Library Washington, D.C. 20234	1 copy
Commanding Officer Office of Naval Research Western Regional Office 1030 East Green Street Pasadena, California 91101	3 copies
Commanding Officer Office of Naval Research Eastern/Central Regional Office 666 Summer Street Boston, Massachusetts 02210	3 copies

Director
U.S. Army Engineering Research
and Development Laboratories
Attn: Technical Documents Center
Fort Belvoir, Virginia 22060 — 1 copy

ODDR&E Advisory Group on Electron Devices
201 Varick Street
New York, New York 10014 — 3 copies

Air Force Office of Scientific Research
Department of the Air Force
Bolling AFB, D.C. 22209 — 1 copy

Air Force Weapons Laboratory
Technical Library
Kirtland Air Force Base
Albuquerque, New Mexico 87117 — 1 copy

Air Force Avionics Laboratory
Air Force Systems Command
Technical Library
Wright-Patterson Air Force Base
Dayton, Ohio 45433 — 1 copy

Lawrence Livermore Laboratory
Attn: Dr. W.F. Krupke
University of California
P.O. Box 808
Livermore, California 94550 — 1 copy

Harry Diamond Laboratories
Technical Library
2800 Powder Mill Road
Adelphi, Maryland 20783 — 1 copy

Naval Air Development Center
Attn: Technical Library
Johnsville
Warminster, Pennsylvania 18974 — 1 copy

Naval Weapons Center
Technical Library (Code 753)
China Lake, California 93555 — 1 copy

Naval Training Equipment Center
Technical Library
Orlando, Florida 32813 — 1 copy

Naval Underwater Systems Center
Technical Center
New London, Connecticut 06320 — 1 copy

Commandant of the Marine Corps — 1 copy
Scientific Advisor (Code RD-1)
Washington, D.C. 20380

Naval Ordnance Station — 1 copy
Technical Library
Indian Head, Maryland 20640

Naval Postgraduate School — 1 copy
Technical Library (Code 0212)
Monterey, California 93940

Naval Missile Center — 1 copy
Technical Library (Code 5632.2)
Point Mugu, California 93010

Naval Ordnance Station — 1 copy
Technical Library
Louisville, Kentucky 40214

Commanding Officer — 1 copy
Naval Ocean Research & Development Activity
Technical Library
NSTL Station, Mississippi 39529

Naval Explosive Ordnance Disposal Facility — 1 copy
Technical Library
Indian Head, Maryland 20640

Naval Ocean Systems Center — 1 copy
Technical Library
San Diego, California 92152

Naval Surface Weapons Center — 1 copy
Technical Library
Silver Spring, Maryland 20910

Naval Ship Research and Development Center — 1 copy
Central Library (Code L42 and L43)
Bethesda, Maryland 20084

Naval Avionics Facility — 1 copy
Technical Library
Indianapolis, Indiana 46218